

Enhanced Robust Altitude Controller via Integral Sliding Modes Approach for a Quad-Rotor Aircraft: Simulations and Real-Time Results

Iván González-Hernández · Sergio Salazar · A. E. Rodríguez-Mata ·
Filiberto Muñoz-Palacios · Ricardo López · Rogelio Lozano

Abstract An enhanced robust altitude control scheme that indicates the improved performance than the typical sliding mode technique for a Quad-rotor air-craft vehicle is proposed in this article by including an integral action in the sliding mode control architecture in order to eliminate the steady-state error induced by the boundary layer and achieving asymptotic convergence to the desired altitude with continuous control input. The proposed integral sliding mode controller is chosen to ensure the stability and robustness of overall dynamics during the altitude control at a desired height reference on the z-axis. Furthermore, we propose a Control Lyapunov Function (CLF) via Lyapunov theory in order to construct the robust stabilizing controller and demonstrate the stability of the z-dynamics of our system. A suitable sliding manifold is designed to achieve the control objective. At last, the simulations and experimental studies are supported by different tests to demonstrate the robustness and effectiveness of the proposed enhanced robust altitude control scheme subject to bounded external disturbances in outdoor environment.

Keywords Integral sliding mode control · Sliding mode technique · Robust altitude control · Nonlinear altitude control Quad-rotor aircraft · Embedded control system

1 Introduction

At present, the major advancements in the control of motion systems are due to the automatic control

theory. The complexity of nonlinear feedback control challenges us to come up with systematic design procedures to meet control objectives and design specifications in scientific projects and research work. Nonlinear control is one of the biggest challenges in modern control theory [2–4]. It is well known that physical systems are nonlinear in nature. Uncertainties, time varying parameters, and input and output disturbances are important to challenge and these necessitate to use nonlinear control methods to design nonlinear controllers. Faced with such challenge, it is clear that we cannot expect one particular procedure to apply to all nonlinear systems. It is also unlikely that the hole design of a nonlinear feedback controller can be based on one particular tool. What a control engineer needs is a set of analysis and design tools that cover a wide range of situations. When working a particular application, the engineer will need to employ the tools that are most appropriate for the problem in hand. In this context, the sliding mode control which is a popular technique among control engineer practitioners is used due to the fact that introduces robustness to unknown bounded perturbations [6, 8–10].

A simple approach to robust control, and the main topic of this article, is the so-called sliding mode control methodology. For the class of systems to which it applies (for instance, air, land and sea vehicles) sliding controller design provides a systematic approach to the problem of maintaining stability and consistent performance in the face of modeling imprecisions. Furthermore, by allowing the trade-offs between modeling and performance to be quantified in a simple fashion, it can illuminate the whole design process [15].

Sliding control has been successfully applied to robot manipulators, high-performance electric motors, underwater vehicles and Unmanned Aerial Vehicle (UAV). Unfortunately, an ideal sliding mode controller has a discontinuous switching function and it is assumed that the control signal can be switched from one value to another infinitely fast. In practical systems, it is impossible to achieve infinitely fast switching control because of finite time delays for the control computation and limitations of physical. Due to imperfect switching in practice it raises the issue of chattering which is highly undesirable. It appears as a high frequency oscillation near the desired equilibrium point and may excite the

unmodelled high-frequency dynamics of the system. Due to these disadvantages of this control strategy it aims to add an integral action to this technique which results in the so well known *integral sliding mode control*. This type of strategy solves the problem in that the system trajectories start in the sliding surface from the first time instant [11–14].

As we know, the altitude control aerial vehicles is a very important point to highlight in particular when someone requires carry out tasks of supervision or aerial surveillance. There are very few works done, so far, in the areas of altitude determination, altitude prediction, and altitude control for Quad-rotors aircraft. During this time, it has been difficult to obtain reference material that provided a comprehensive overview of robust altitude controls. This lack of reference material has made it difficult for those not intimately involved in altitude functions to become acquainted with the ideas and activities which are essential to understanding the various aspects of spacecraft altitude support. Today, there exists insufficient literature about the problem of the altitude control design using integral sliding mode in the area of quadrotors. For instance, in the work by Nonaka and Sugizaki [5], an integral sliding mode altitude control for a small model helicopter with ground effect compensation is proposed. The authors then present the implementation of an integral action on a robust control based on sliding modes for a conventional helicopter but the disadvantage of this type of platform is its complex structure which is constituted meanwhile in [6] the author has proposed a method to improve the altitude control of the Quad-rotor aircraft, using Sliding Mode Control for both translational and rotational dynamics of the Quad-rotor. This approach is based on implementing a smoothed *sign* function utilizing the approximation $sign(s) \approx \frac{s}{|s|+\varepsilon}$ where $\varepsilon > 0$. Since the sliding mode entails $s \approx 0$, the noise in the observed quantities becomes highly effective and the controller can generate unnecessarily large control signals. This is known as the chattering in the related literature [3]. Utilizing the above approximation introduces a boundary layer and eliminates the undesired chattering phenomenon significantly.

The primary purpose of this paper is to provide an enhanced robust altitude controller using sliding mode where an integral action has been added in order to eliminate the steady-state error in the Quad-rotor aircraft to reach a desired altitude in outdoor environment.

Afterwards, the robust altitude controller is formulated and programming in real-time using an autopilot of last generation with all the instrumentation required to integrate the altitude control algorithm that corresponding. It also has been chosen for its insensitivity to the model errors, parametric uncertainties and external disturbances. Moreover, the vehicle built to test this robust altitude controller is shown in Fig. 1. Finally, some simulations and experimental studies are presented in order to compare this enhanced robust altitude algorithm with the traditional and conventional sliding mode control in dynamic responses of the closed-loop control system.

This paper is organized as follows: Section 2 presents the dynamical model of the Quad-rotor aircraft by Euler-Lagrange approach. The enhanced robust altitude control algorithm using sliding mode with integral action and the corresponding stability analysis is presented in Section 3. The effectiveness of this controller proposed to the robust altitude control is evaluated and compared through of different simulations in Section 4 whereas in Section 5 experimental results from tests performed outdoor are evaluated. Finally, in Section 6 the conclusions are drawn.

2 Quadrotor Aircraft Modeling

In this section, the general dynamic model of a Quadrotor aircraft is presented. To start, a Quadrotor aircraft is a complex system that is lifted and propelled by four rotors. This type of aerial vehicles can be controlled by varying the relative speed

of each rotor to change the thrust and torque produced by each. Quadrotors are classified as rotorcraft, as opposed to fixedwing aircraft, because their lift is derived from four rotors. The use of four rotors allows each individual rotor to have a smaller diameter than the equivalent single-rotor helicopter, allowing them to store less kinetic energy during flight and thus reduces the damage caused by the rotors hitting any objects. By enclosing the rotors within a frame, the rotors can be protected during collisions. In this type of vehicles, vertical motion is created by collectively increasing and decreasing the speed of all four rotors; pitch or roll motion is achieved by the differential speed of the front-rear set or the left-right set of rotors, coupled with lateral motion; yaw motion is realized by the different reaction torques between the (1,3) and (2,4) rotors as shown in Fig. 2.

Let $\mathcal{I} = \{i_I, j_I, k_I\}$ be the inertial frame, $\mathcal{B} = \{i_B, j_B, k_B\}$ denote a set of coordinates fixed to the rigid aircraft as is shown in Fig. 2. Let $q = (x, y, z, \phi, \theta, \psi)^T \in \mathbb{R}^6 = (\xi, \eta)^T$ be the generalized coordinates vector which describe the position and orientation of the flying machine, so the model could be separated in two coordinate subsystems: translational and rotational. They are defined respectively by

- $\xi = (x, y, z)^T \in \mathbb{R}^3$: denotes the position of the vehicle's mass center relative to the inertial frame \mathcal{I} .
- $\eta = (\phi, \theta, \psi)^T \in \mathbb{R}^3$: describe the orientation of the aerial vehicle, *i.e.* roll, pitch and yaw angles respectively.

Fig. 1 The Quadrotor aircraft experimental platform with embedded control system





Fig. 2 The Quadrotor aircraft frames scheme

The model of the full Quadrotor aircraft (see [1]) is obtained from the Euler-Lagrange equations with external generalized force F_B and generalized moment τ_η where F_I is the translational force applied to the Quad-rotor aircraft due to the control input. Then

$$F_B = (0, 0, u)^T \quad (1)$$

where u is the sum of mechanical thrust forces: $u = f_1 + f_2 + f_3 + f_4$ with $f_i = k_i \omega_i^2$ for $i=1,2,3,4$, $k_i > 0$ is a constant and ω_i is the angular speed of motor i , as

shown in Fig. 2. This force vector can be expressed in the inertial frame as

$$F_I = R^{B \rightarrow I} F_B \quad (2)$$

where $R^{B \rightarrow I}$ is the transformation of vectors from the body-fixed frame to the earth-fixed frame based on Euler angles and the rotation matrix defined by

$$R^{B \rightarrow I} = \begin{pmatrix} c_\theta c_\psi & s_\psi c_\theta & -s_\theta \\ c_\psi s_\theta s_\phi - s_\psi c_\phi & s_\psi s_\theta s_\phi + c_\psi c_\phi & c_\theta s_\phi \\ c_\psi s_\theta c_\phi + s_\psi s_\phi & s_\psi s_\theta c_\phi - c_\psi s_\phi & c_\theta c_\phi \end{pmatrix} \quad (3)$$

The generalized moments on the η variables are denoted by $\tau_\eta = (\tau_\phi \ \tau_\theta \ \tau_\psi)^T$ where

$$\begin{aligned}\tau_\phi &= (f_3 - f_1)l \\ \tau_\theta &= (f_2 - f_4)l \\ \tau_\psi &= ((f_1 + f_2) - (f_3 + f_4))d\end{aligned}\quad (4)$$

where l is the distance to the center of gravity and d is the drag coefficient produced by coordinated reactive torque involving the four rotors because of the geometry of the Quad-rotor aircraft. Since the lagrangian contains no cross terms in the kinetic energy, combining $\dot{\xi}$ and $\dot{\eta}$ vectors in the Euler-Lagrange equation can be partitioned into the dynamics for the ξ coordinates and the η dynamics. So, we obtain

$$\begin{aligned}F_{\mathcal{L}} &= m\ddot{\xi} + mg \\ \tau_\eta &= J\ddot{\eta} + \dot{J}\dot{\eta} - \frac{1}{2} \frac{\partial}{\partial \eta} (\dot{\eta}^T J \dot{\eta})\end{aligned}\quad (5)$$

Defining the Coriolis terms and gyroscopic and centrifugal terms as

$$C(\eta, \dot{\eta})\dot{\eta} = \dot{J}\dot{\eta} - \frac{1}{2} \frac{\partial}{\partial \eta} (\dot{\eta}^T J \dot{\eta})\quad (6)$$

Finally, the dynamic model of the Quad-rotor aircraft is the following

$$\begin{pmatrix} m\ddot{x} \\ m\ddot{y} \\ m\ddot{z} \end{pmatrix} = \begin{pmatrix} -u \sin \theta \\ u \sin \phi \cos \theta \\ u \cos \phi \cos \theta \end{pmatrix} + \begin{pmatrix} 0 \\ 0 \\ -mg \end{pmatrix}\quad (7)$$

$$J\ddot{\eta} = \tau_\eta - C(\eta, \dot{\eta})\dot{\eta}\quad (8)$$

where x and y are the coordinates in the horizontal plane and z is the vertical position, whereas that ϕ is the roll angle around the x -axis, θ is the pitch angle around the y -axis and ψ is the yaw angle around the z -axis. The control input u and the vector $\eta = (\phi, \theta, \psi)^T$ are the total thrust or collective input and the angular moments, respectively. Finally, J is the inertia tensor and C is the Coriolis force acting on the Quad-rotor aircraft.

3 Nonlinear Control Design

In this section we present a robust control law to stabilize the aerial vehicle to desired altitude. We will first present the enhanced robust altitude control which is based on sliding-mode technique with the integral action added. We then propose a *pose* control

algorithm to keep the quadrotor aircraft in a fixed position in order to ensure the proper altitude control performance at a stationary point.

3.1 Enhanced Robust Altitude Control

Since altitude control concerns only in the dynamics of the z -axis, we can consider the z -dynamic described in Eq. 7, where

$$\ddot{z} = \frac{1}{m} (u \cos \phi \cos \theta - mg)\quad (9)$$

or we can have the following state space variable set,

$$\begin{aligned}\dot{z}_1 &= z_2 \\ \dot{z}_2 &= \frac{1}{m} (u \cos \phi \cos \theta - mg)\end{aligned}\quad (10)$$

To start, the design problem is to enforce the behavior of the system states towards the desired trajectories, which are known. Denote the reference trajectories by \dot{z}_d and z_d which is velocity and altitude desired respectively. Afterwards, we define the tracking errors by $e_z = z - z_d$, $\dot{e}_z = \dot{z} - \dot{z}_d$ and $\ddot{e}_z = \ddot{z} - \ddot{z}_d$ where z_d is the desired altitude.

3.2 Integral Sliding Mode Controller

First of all, the *sliding mode control with integral action* scheme introduces a “*sliding surface*” along which the sliding motion is to take place. This surface is denoted by s and is defined as follow

$$\begin{aligned}s &= \left(\frac{d}{dt} + \lambda\right) e_z + k_I \int_0^\infty e_z dt \\ s &= \dot{e}_z + \lambda e_z + k_I \int_0^\infty e_z dt\end{aligned}\quad (11)$$

where $\lambda > 0$ is the slope of the sliding line and k_I is the integral gain. And the derivative of the sliding surface in Eq. 11 can be given as

$$\dot{s} = \ddot{e}_z + \lambda \dot{e}_z + k_I e_z\quad (12)$$

3.3 Stability Analysis

In order to provide stability about the equilibrium point, we propose the following Lyapunov function candidate as

$$V = \frac{1}{2} s^2\quad (13)$$

The time derivative of the Lyapunov function candidate in Eq. 13 can be computed as follows

$$\dot{V} = s\dot{s} \quad (14)$$

then, doing the mathematical operations corresponding, we have that

$$\begin{aligned} \dot{V} &= s(\ddot{z} + \lambda\dot{z} + k_I e_z) \\ \dot{V} &= s(\ddot{z} - \ddot{z}_d + \lambda(\dot{z} - \dot{z}_d) + k_I(z - z_d)) \end{aligned} \quad (15)$$

after, we need that $\ddot{z}_d = 0$ and $\dot{z}_d = 0$ therefore

$$\dot{V} = s(\ddot{z} + \lambda\dot{z} + k_I(z - z_d)) \quad (16)$$

then, substituting Eq. 9 in Eq. 16 leads to

$$\dot{V} = s \left(\frac{1}{m} (u \cos \phi \cos \theta - mg) + \lambda\dot{z} + k_I(z - z_d) \right) \quad (17)$$

Also, we can consider presence of bounded disturbances $f(z, \dot{z})$, as follows

$$\dot{V} = s \left(\frac{1}{m} (u \cos \phi \cos \theta - mg) + \lambda\dot{z} + k_I(z - z_d) + f(z, \dot{z}) \right) \quad (18)$$

where we have to drive the variable s in Eq. 11 to zero in finite time by means of the control u . Therefore, assuming that

$$u = \frac{m(-\lambda\dot{z} - k_I(z - z_d) + mg)}{\cos \phi \cos \theta} + v \quad (19)$$

and substituting it into Eq. 18 we obtain

$$\dot{V} = s(f(z, \dot{z}) + v) = sf(z, \dot{z}) + sv \leq |s|L + sv \quad (20)$$

then

$$\dot{V} \leq |s|L + sv \quad (21)$$

selecting

$$v = -\rho \operatorname{sign}(s) \quad (22)$$

where $\rho > 0$ and $\operatorname{sign}(s) = \frac{s}{|s|}$ substituting into Eq. 21 we obtain

$$\dot{V} \leq |s|L + s \left(-\rho \frac{s}{|s|} \right) = |s|L - |s|\rho \quad (23)$$

therefore

$$\dot{V} \leq -|s|(\rho - L) \quad (24)$$

Therefore, the robust control law u_z proposed below will drive the Quad-rotor aircraft to the desired altitude,

$$u_z = \frac{m(u_{SMC} + mg)}{\cos \phi \cos \theta} \quad (25)$$

if and only if

$$\rho > L \quad (26)$$

where L is the upperbound of the external perturbation. This condition ensures a stable performance of the altitude control for the Quad-rotor aircraft in z - axis at a desired altitude. For simplicity the term u_{SMC} includes the sliding mode action which is described as:

$$u_{SMC} = -\lambda\dot{z} - k_I(z - z_d) - \rho \operatorname{sign}(s) \quad (27)$$

From control law (25) described above, it follows that the pitch and roll angles must belong to $\phi, \theta \in (-\frac{\pi}{2}, \frac{\pi}{2})$ in order to avoid singular positions, which represents a real situation in hover flight. Then, using Eq. 25 into Eq. 9 we get

$$\ddot{z} = -\lambda\dot{z} - k_I(z - z_d) - \rho \operatorname{sign}(s) \quad (28)$$

choosing the correct values of λ , k_I and ρ in Eq. 28 ensures a stable performance of the altitude of the Quad-rotor aircraft.

3.4 Position Control

A two-level control is used to stabilize the position of the aerial vehicle. Let us consider the dynamics

Table 1 Simulations parameters for sliding mode control

Parameters	Value
Mass of the Quad-rotor aircraft, (m) [kg]	1.1
Gravitational acceleration, (g) [m/s^2]	9.81
Reaching law parameter, (ρ)	0.80
Slope parameter, (λ)	1.20
Integral gain, (k_I)	0.02

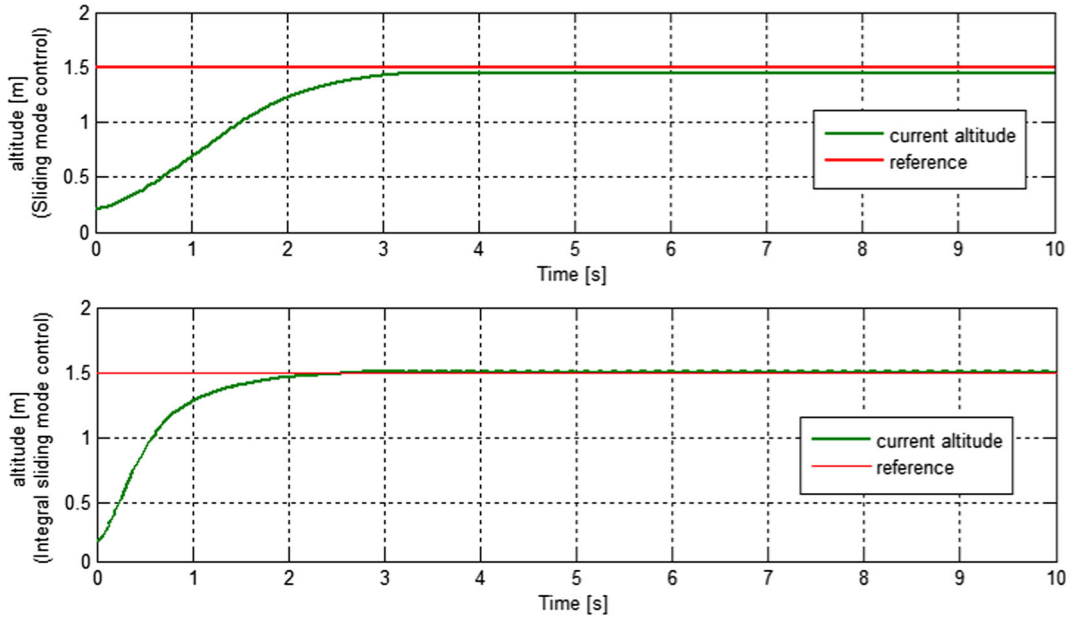


Fig. 3 Altitude *Sliding Mode Control* and *Integral Sliding Mode* signals comparison

in Eq. 7 which describe the horizontal motion of the quadrotor aircraft. So, introducing (25) into the horizontal dynamics of Eq. 7 and assuming that c_1 is small enough means that the vehicle has achieved the required altitude and hence this variable $c_1 \rightarrow 0$ for a time T , then the dynamics in the axis x and y is represented for the following expressions,

$$\ddot{x} \approx -g \frac{\tan \theta}{\cos \phi} \quad (29)$$

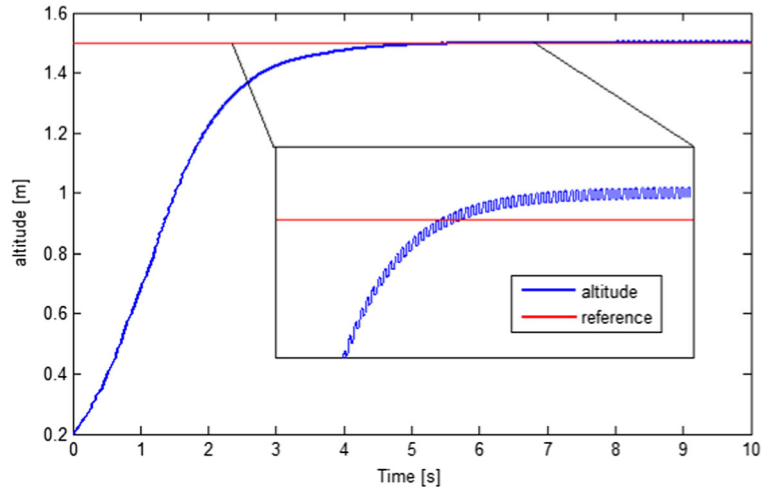
$$\ddot{y} \approx g \tan \phi \quad (30)$$

For the approximate model given by Eqs. 29–30, ϕ and θ are the corresponding control inputs of the system. These control inputs also represent the trajectories to be tracked in order to regulate the horizontal motion, therefore let us define the desired trajectory as

$$\theta_d = \arctan\left(\frac{u_x \cos \phi}{g}\right) \quad (31)$$

$$\phi_d = \arctan\left(\frac{u_y}{g}\right) \quad (32)$$

Fig. 4 *Altitude Sliding Mode Control* response. There exists steady-state error



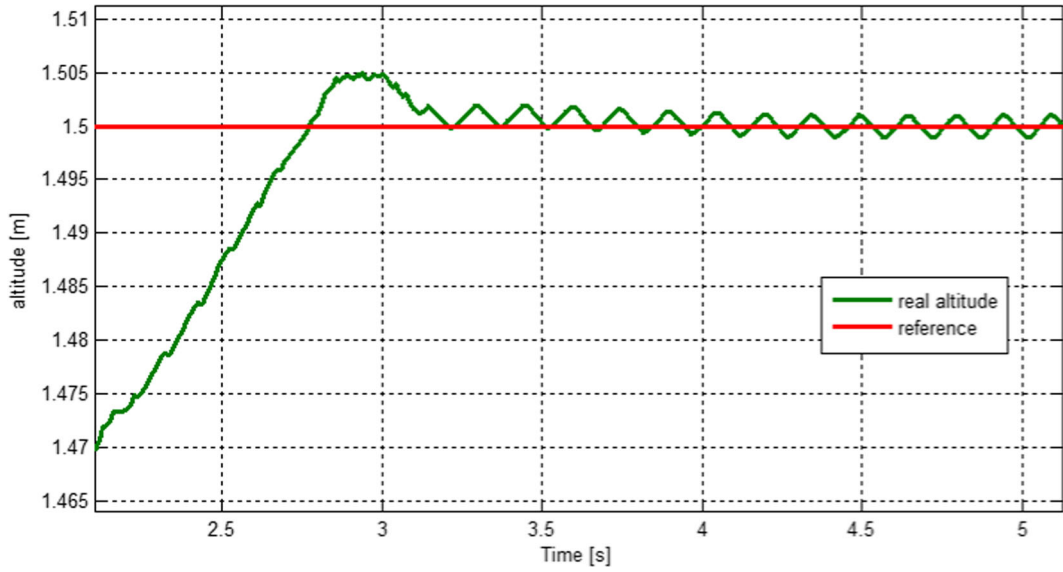


Fig. 5 Altitude Sliding Mode Control with integral action response. There no exists steady-state error

where

$$u_x = -k_{p_x}x - k_{v_x}\dot{x}$$

$$u_y = k_{p_y}y + k_{v_y}\dot{y}$$

with $k_{p_x}, k_{v_x} > 0$ and $k_{p_y}, k_{v_y} > 0$. The above expressions represent a conventional PD controller. Notice that, the measurements of position and velocity

translational which the controller consists are directly acquired by the GPS module. Finally, the state feedback controls Eqs. 32 and 31 will transform the approximate horizontal dynamic model (29)–(30) into

$$\ddot{x} = u_x \quad (33)$$

$$\ddot{y} = u_y \quad (34)$$

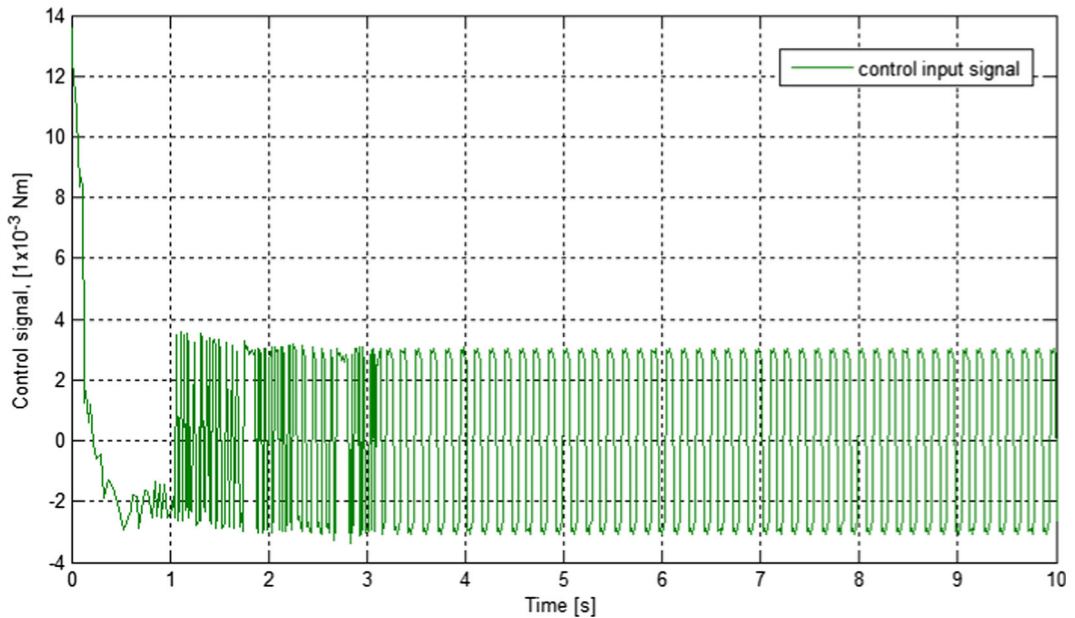


Fig. 6 Control input signal response applied to the Quadrotor aircraft

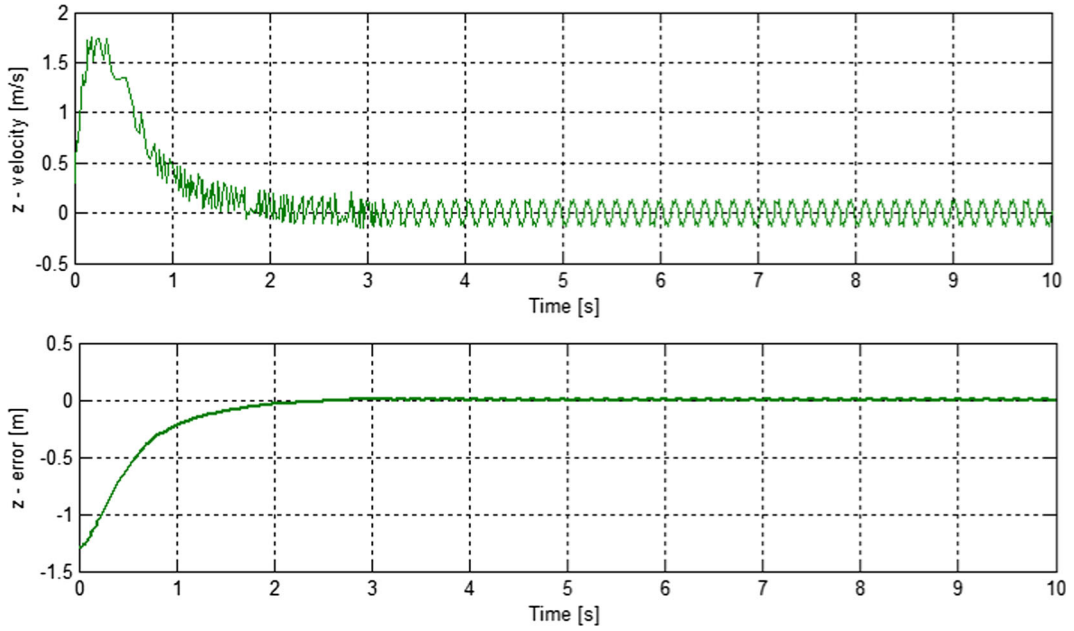


Fig. 7 Velocity signal and resulting error when applying the *Sliding Mode Control with integral action*

assuming that $\theta = \theta_d$ and $\phi = \phi_d$, respectively.

3.5 Attitude Control

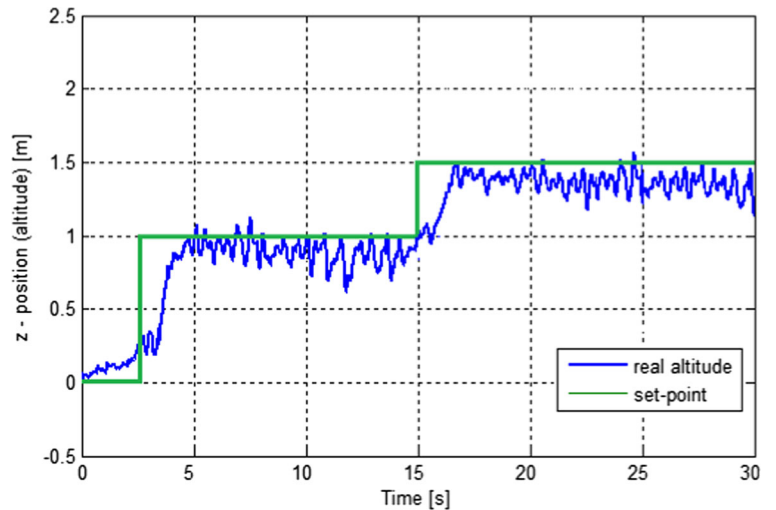
The yaw angular position $\ddot{\psi}$ can be controlled by applying

$$\tau_\psi = -a_{\psi_1} \dot{\psi} - a_{\psi_2} (\psi - \psi_d) \quad (35)$$

where ψ_d is the desired yaw angular position. Now, we propose a control law using saturation function in [7] for the *roll and pitch control*. This control law is used to avoid abrupt behavior in the performance of the Quadrotor aircraft.

$$\begin{aligned} \tau_\phi = & -\sigma_{\phi_1} (k_1 \phi_2 + \sigma_{\phi_2} (k_2 (\phi_2 + k_1 \phi_1) \\ & + \sigma_{\phi_3} (k_3 ((\phi_2 + k_1 \phi_1) + k_1 k_2 y_2 + k_2 \phi_1) \\ & + \sigma_{\phi_4} (k_4 ((\phi_2 + k_1 \phi_1) + k_1 k_2 y_2 + k_2 \phi_1) \\ & + k_3 \phi_1 + k_1 k_2 k_3 y_1 + (k_1 + k_2) k_3 y_2))) \end{aligned} \quad (36)$$

Fig. 8 Real-time *altitude sliding mode control* response of the Quadrotor aircraft. There exists steady-state error



and

$$\begin{aligned} \tau_\theta = & -\sigma_{\theta_1} (k_1\theta_2 + \sigma_{\theta_2} (k_2 (\theta_2 + k_1\theta_1) \\ & + \sigma_{\theta_3} (k_3 ((\theta_2 + k_1\theta_1) - k_1k_2x_2 + k_2\theta_1) \\ & + \sigma_{\theta_4} (k_4 ((\theta_2 + k_1\theta_1) - k_1k_2x_2 + k_2\theta_1) \\ & + k_3\theta_1 - k_1k_2k_3x_1 - (k_1 + k_2)k_3x_2))) \end{aligned} \quad (37)$$

where $\sigma(s)$ is a saturation function is defined as

$$\sigma(s) = \begin{cases} M & \text{if } s > M \\ s & \text{if } -M \leq s \leq M \\ -M & \text{if } s < -M \end{cases} \quad (38)$$

Therefore, the three previous controls (*altitude, attitude and position*) ensure a favorable performance to execute the tests of the outdoor enhanced robust altitude algorithm in order to verify the efficiency of the quadrotor vehicle in an autonomous flight for a given altitude reference.

4 Simulations Results

In this section, we present the results obtained from a few simulations using the proposed sliding mode controller with integral action against conventional sliding mode control. A short list of the parameters of the integral sliding mode control law used in these simulations are briefly described in Table 1.

In the simulations, some external disturbances has been introduced to test stability robustness in the

Sliding Mode technique for the altitude control of the Quad-rotor aircraft.

4.1 Altitude Simulation Results

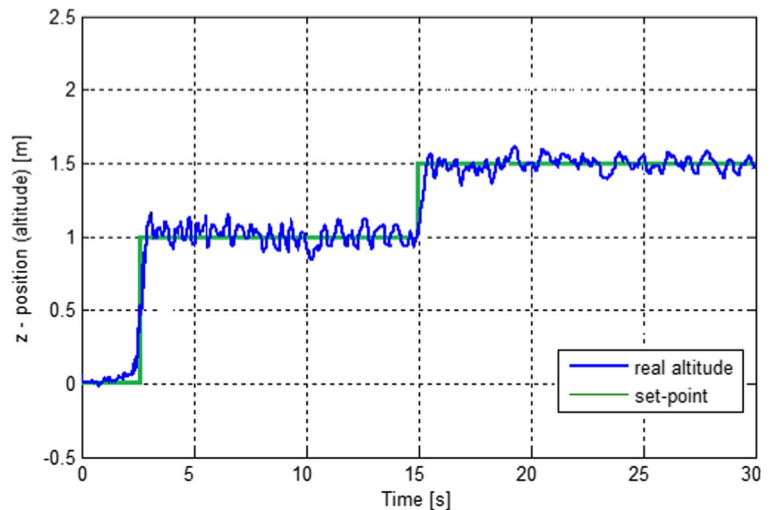
The results of the simulation of the altitude control based on sliding mode conventional and with integral action are shown in Figs. 3, 4 and 5. Moreover, a bounded disturbance (d) of the way

$$d(t) = 0.15 \sin(0.15t)$$

has been introduced to test the efficiency of the proposed robust control algorithm. Figure 3 details the comparison between a conventional sliding mode and integral action added. Notice that the convergence of the current altitude of the aerial vehicle towards the provided reference is faster in the sliding mode with integral action than sliding mode conventional which means better performance. On the other hand, Fig. 4 illustrates a sliding mode control example for a desired altitude. The target is at 1.5 meters but there exists a steady-state error in the current altitude. Meanwhile in Fig. 5 we can observe that the Quadrotor aircraft is able to arrive at the reference without the steady-state error in the current altitude which shows a good performance of the proposed technique.

In addition, Figs. 6 and 7 show additional information the control input (*sliding mode control with integral action*) applied to the Quadrotor aircraft to carry an altitude of 1.5m as well as the resultant velocity on the dynamics in the z-axis and the

Fig. 9 Real-time *altitude integral sliding mode control* response of the Quadrotor aircraft. There no exists steady-state error



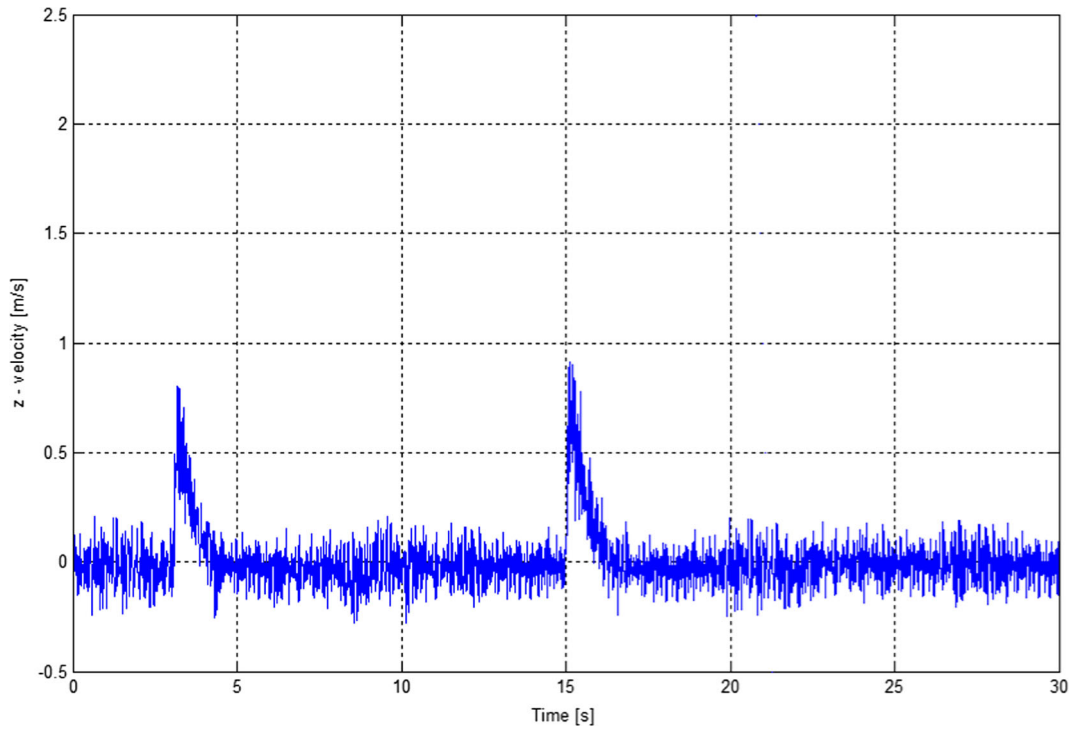


Fig. 10 Velocity signal response using the integral sliding mode control

asymptotic convergence error to zero which implies the proper operation of the controller. It is worth noting that, if a faster convergence is required only needs to increase the controller gains although in a real-time application can vary too much depending on the weight and distribution of the components in the aerial vehicle.

5 Real-Time Implementation and Results

In this section we present the results obtained when applying the enhanced robust altitude control law based on integral sliding mode proposed in the nonlinear control design. For this objective, we use the Quadrotor aircraft built (see Fig. 1), with a Futaba 2.4GHz

Fig. 11 Control input signal applied to the Quadrotor aircraft using the conventional sliding mode control

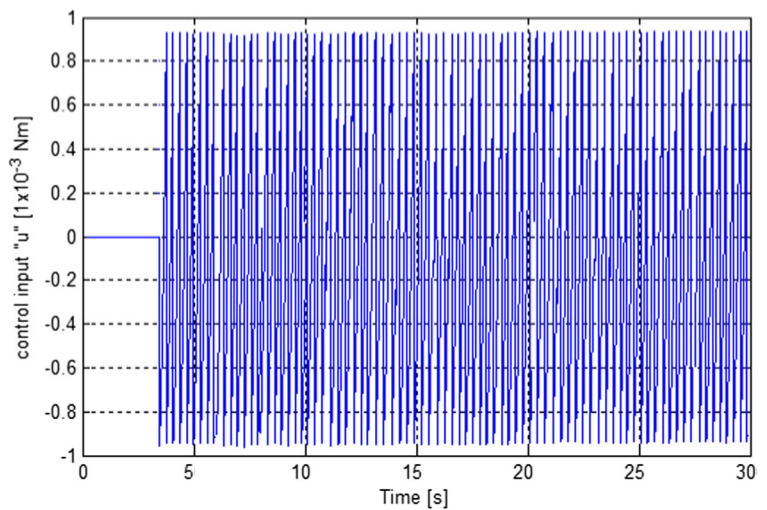
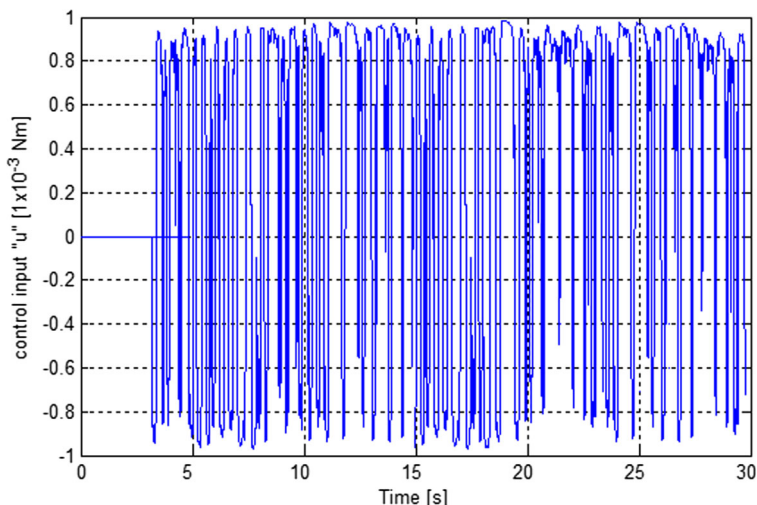


Fig. 12 Control input signal applied to the Quadrotor aircraft using the integral sliding mode control



FASST radio system for transmitting the control signal to activate the automatic mode and start running the robust altitude control algorithm. In order to measure the position (x, y) and the attitude (ϕ, θ, ψ) of the Quad-rotor aircraft, we use the high-performance autopilot-on-module system (*pixhawk*) with an u-blox GPS module sensor. The benefits of the Pixhawk system include integrated multithreading, a Unix/Linux-like programming environment for real-time applications. While for *altitude measurement* (z), we use the precision micro-barometer module MS5611. This device is a high precision barometric pressure sensor which includes a linear pressure measurement element and

an ultra-low power 24-bit ($\Sigma\Delta$) A/D-converter with internal factory calibrated coefficients. The main function is to convert the proportional analogue voltage from the pressure measured to a 24-bit digital value, as well as providing a 24-bit value for the temperature. These values allow to obtain a resolution of 10cm thanks to the high-sensitivity that has to register a minimum change in the altitude measured. Also, the sensing principle employed leads to very low hysteresis and high stability of both pressure and temperature signal. To perform the test of the altitude control, we have the next initial conditions $(z, \dot{z}) = (0, 0)$ where we consider a reference altitude of 1.5m with a wind

Fig. 13 Sliding surface signal obtained applying the typical sliding mode control

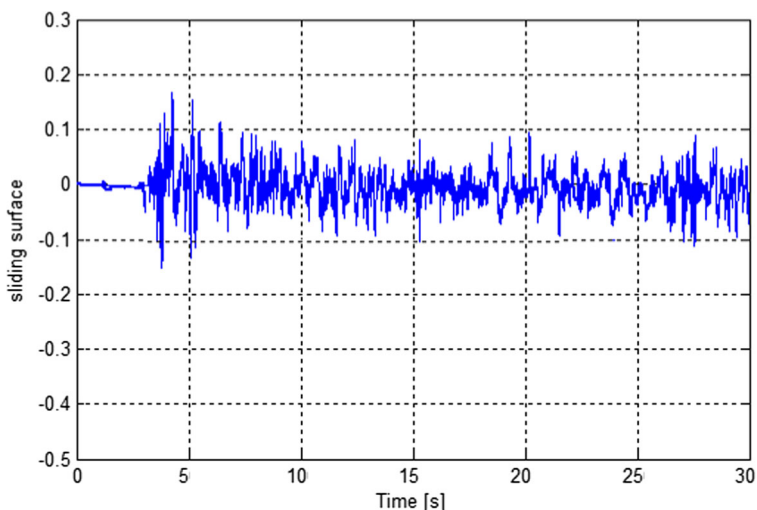
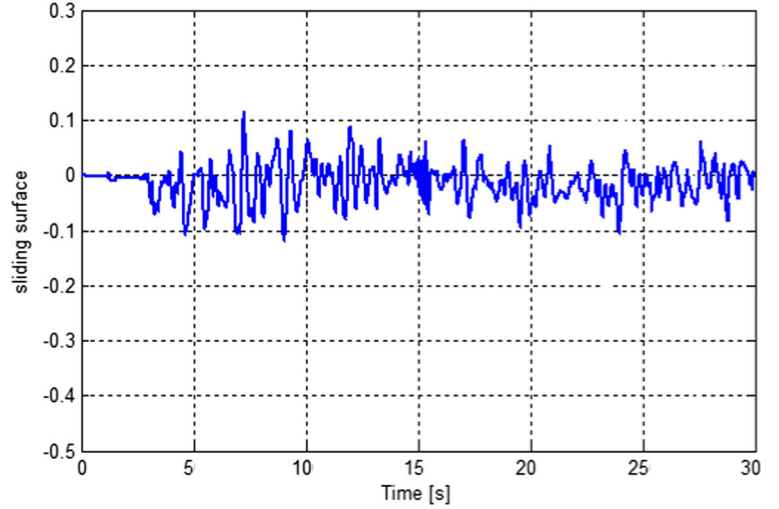


Fig. 14 Sliding surface signal obtained applying the integral sliding mode control



speed at about of $3m/s$ (weather conditions at the time of the test). Figures 8, 9, 10, 11, 12, 13 and 14 present the experimental results obtained by applying the altitude control using conventional and integral sliding mode technique. Parameters of this aerial vehicle are given in Table 2.

To start, Figs. 8 and 9 show a comparison of control performance for two different setpoints, the first one of $1m$ at time $t = 2.5s$ and the second of $1.5m$ at time $t = 15s$ using the conventional and integral sliding mode control, respectively. Notice that, it has reduced the steady-state error which is the main objective to be achieved with this technique enhanced control. Both figures show the development of the same instants experiments to demonstrate the efficiency of a technique against each other, respectively. Clearly, we can see an improvement in the altitude control response to reach the desired reference in the Quadrotor aircraft

due to embedded high-resolution barometric pressure sensor implemented which presents an approximate error of $\pm 5cm$ of error when carrying out the test flight. There is also an increase in the arrival of the aerial vehicle at intervals $t = 2.5s$ and $t = 15s$ for the assigned references. Then, with respect to Fig. 10 we can see the behavior of the linear velocity (z-axis) produced by running the test flight in the two set-points previously described for the time instants $t = 2.5s$ and $t = 15s$ where one can clearly observe the two velocities increments that correspond precisely to the instants in which the helicopter changes its altitude following the current reference. Notice that, the fast convergence to zero of the velocity signal demonstrates the efficiency of the added integral action in the altitude sliding mode control employed.

Meanwhile Figs. 11 and 12 show the control signals applied to the Quadrotor aircraft using these two control techniques. As in the previous case, we can observe as the control signal obtained by the integral sliding mode control is smoother than that obtained with the conventional sliding mode control which means higher performance of the actuators (in this case; brushless motors) for good long-term operation.

Finally, Figs. 13 and 14 show as additional data the sliding surfaces generated by two control techniques, respectively. That may be of interest to observe the evolution of the response time of both controllers. Similarly, we can see a softer signal obtained by the conventional sliding mode technique but with integral action added.

Table 2 Integral Sliding Mode Control parameters

Parameters	Value
Mass of the Quad-rotor aircraft, (m) [kg]	1.2
Gravitational acceleration, (g) [m/s^2]	9.81
Reaching law parameter, (ρ)	0.95
Slope parameter, (λ)	1.3
Integral gain, (k_I)	0.045
I_{xx} , [$kg \cdot m_2$]	0.0039
I_{yy} , [$kg \cdot m_2$]	0.0041
I_{zz} , [$kg \cdot m_2$]	0.0071



Fig. 15 The Quadrotor aircraft flying at a particular altitude using integral sliding mode control autonomously

6 Conclusions

In this article, an enhanced robust altitude control based on integral sliding mode strategy for a Quadrotor aircraft has been proposed in order to eliminate the steady-state error in a desired altitude reference in an autonomous flying (Fig. 15). This control law was experimentally demonstrated in real-time under external perturbations such as little wind gusts. We also developed several simulations to find approximate gains for tuning the control algorithm programmed into the embedded control system and validate the robustness of the altitude algorithm proposed under the weather conditions that were presented at the time of outdoor testing. Using a control Lyapunov function was possible to obtain the robust altitude control law to stabilize the aerial vehicle and improve the response time to the desired altitude. Notice that, the quadrotor aircraft platform was built to perform the different experiments to demonstrate the efficiency of the robust altitude control. Finally, we consider that the altitude control is an important issue to execute critical tasks such as the landing and take-off of this kind of aircrafts.

References

1. Lozano, R. (ed.): *Unmanned Aerial Vehicles: Embedded Control*. John Wiley & Sons, Hoboken (2010)
2. Khalil, H.K.: *Nonlinear systems*. Prentice Hall (2002)
3. Slotine, J.J., Li, W.: *Applied Nonlinear Control*. Prentice-Hall, New Jersey (1991)
4. Edwards, C., Spurgeon, S.: *Sliding mode control: theory and applications* Taylor & Francis (1998)
5. Nonaka, K.: H Sugizaki, Integral Sliding Mode Altitude Control for a Small Model Helicopter with Ground Effect Compensation, in *American Control Conference*, 202–207 (2011)
6. Efe, M.O.: Robust Low Altitude Behavior Control of a Quadrotor Rotorcraft Through Sliding Modes. In: *Mediterranean Conference on Control and Automation*, pp. 1–6 (2007)
7. González, I., Salazar, S., Lozano, R.: Chattering-Free Sliding Mode Altitude Control for a Quad-Rotor Aircraft: Real-Time Application. In: *J. Intell. Robot. Syst.*, vol. 73, pp. 137–155 (2013)
8. Benallegue, A., Mokhtari, A., L Fridman, Feedback linearization and high order sliding mode observer for a Quadrotor UAV. In: *International Workshop on Variable Structure Systems*, pp. 365–370 (2006)
9. Bouabdallah, S., Siegwart, R.: Backstepping and sliding-mode techniques applied to an indoor micro Quadrotor. In: *IEEE International Conference on Robotics and Automation*, pp. 2259–2264 (2005)
10. Xu, R., Ozguner, U.: Sliding mode control of a Quadrotor helicopter. In: *IEEE Conference on Decision & Control*, pp. 4957–4962 (2006)
11. Eker, I., Akinal, S.A.: Sliding mode control with integral action and experimental application to an electromechanical. In: *ICSC congress on computational intelligence methods and applications* (2005)
12. Poznyak, A., Fridman, L., Bejarano, F.: Mini-max integral sliding-mode control for multimodel linear uncertain systems. In: *IEEE Transactions on Automatic Control*, vol. 49, pp. 97–102 (2004)
13. Fridman, L., Poznyak, A., Bejarano, F.: Decomposition of the minmax multi-model problem via integral sliding mode.

In: *International Journal of Robust and Nonlinear Control*, vol. 15, pp. 559–574 (2005)

14. Utkin, V., Shi, J.: Integral sliding mode in systems operating under uncertainty conditions. In: *Proc. 35th IEEE Decision and Control Conf.*, vol. 4, pp. 4591–4596 (1996)
15. Slotine, J.J.E.: Sliding controller design for nonlinear systems. In: *Int. J. Control*, vol. 40, pp. 421–434 (1984)

Iván González-Hernández was born in México City, on March 18, 1981. He received the engineering degree in Communications and Electronics from the Instituto Politécnico Nacional, México City, in 2003, and he achieved his MSc and PhD studies in Automatic Control at the Centro de Investigación y de Estudios Avanzados del I.P.N. (CINVESTAV), México City, in 2009 and 2013, respectively. At present, he works as research professor commissioned in the UMI-LAFMIA 3175 CNRS laboratory through an agreement called Catédra-CONACYT, where his current research interests include real-time control applications, nonlinear control techniques and embedded control systems in Unmanned Aerial Vehicles (UAV) in particular the Quad-rotor aircraft configuration.

Sergio Salazar was born in Tlaxcala, México, on October 7, 1966. He received the B.S. degree in electronics engineering from the Benemérita Universidad Autónoma de Puebla, Puebla, México, in 1992, the M.Sc. degree in electrical engineering from the Centro de Investigación y Estudios Avanzados, Mexico city, Mexico, in 1995, and the Ph.D. degree in automatic control from the University of Technology of Compiegne (UTC), Compiegne, France. From 2010 he is a Professor/researcher at UMI-LAFMIA 3175, Cinvestav-IPN. His current research areas includes Control of under actuated mechanical nonlinear systems, modeling and control of mini aerial vehicles, embedded and real-time systems.

A. E. Rodríguez-Mata received his Chemical Engineering and Master degree at Tecnológico de Estudios Superiores de Ecatepec, México. His thesis focused on applications of catalysis to wastewater treatment processes and robotics systems. He is currently a PhD student at CINVESTAV, México. He currently works as a researcher for CONACYT (National Council of National Science and Technology) in the northwest in México. He is interested in nonlinear control of biological systems, robust control estimation in Robots and the development of research for environmental improvement.

Filiberto Muñoz-Palacios was born in Hidalgo, Mexico, on November 29, 1980. He received the B. Eng. degree in Electronics and Telecommunications and the M.Sc. degree in Automation and Control from the Autonomous University of Hidalgo State, Mexico, in 2004 and 2007 respectively. Since September 2006, he holds a Professor Researcher position with the Mechatronics Department at the Polytechnic University of Pachuca, Hidalgo, México. He is currently a Ph.D. student of the Automatic Control Department in Center for Research and Advanced Studies of the IPN (CINVESTAV). His research interests include Robust Control, Unmanned Aerial Systems and Multi-Agent Systems.

Ricardo López was born in Puebla Mexico, on November 26, 1983. He received the degree bachelor of Science in Electronics with a major in Automatic Control at the Autonomous University of Puebla (BUAP) in 2007 in Puebla, Mexico. He obtained the degree of Master of Science in electronics with option in automation in 2010, in the faculty of electronics, BUAP. He obtained the degree of PHD in automatic control, in the department of automatic control of the CINVESTAV of the National Polytechnic Institute (CINVESTAV) in 2014. His research interest is focused on the design and construction exoskeletons and Robotics applied to rehabilitation include modeling and control of these systems. He is currently works as a professor researcher for CONACYT (National Council of National Science and Technology) at the Joint International Unit (UMI 3175) in the Franco Mexican Laboratory of Computer Science and Automation (LAFMIA) at the unit Zacatenco CINVESTAV.

Rogelio Lozano was born in Monterrey Nuevo Leon on July 12, 1954. Communications and Electronics Engineer in ESIME IPN in 1975, Master of Science in Automatic Control CINVESTAV in 1977 and PhD in Automatic Control of Grenoble INP France in 1981. Professor of the Department of Automatic Control from 1981 to 1989. Since 1990, CNRS Research Director at the Technological University of Compiegne, France. Director of Laboratory Heudiasyc 1995 to 2007. Since 2008 is Director of the Joint International Unit of CINVESTAV LAFMIA, CNRS and CONACYT. His research interests include the design and control of aerial vehicles and unmanned submarines.